Mobile Practice. Best Practice.

PREMIER SPONSOR
ACVS
American College of Veterinary Surgeons

Transform your quality of life and increase access to care as a MOVES mobile surgeon.

- No nights, weekends, or holidays.
- Set your own schedule days.
- Full-time technician/assistant.
- Company-supplied vehicle and all medical & sterilization equip.
- Unlimited paid vacation time.
- Paid parental & maternity leave.
- Equity incentive stock options.
- World-class marketing and business support.

MOVES™

Now hiring small animal surgeons nationwide!

Click to apply now or visit us at www.VetMoves.com for more info.

LEARN MORE

Click to start your discovery and connect with our recruiting team at vetmoves.com/careers/

Received: 30 July 2022 | Revised: 26 October 2022 | Accepted: 26 November 2022

DOI: 10.1111/vsu.13925

WILEY

CLINICAL RESEARCH

Minimally invasive plate osteosynthesis of femoral fractures with 3D-printed bone models and custom surgical guides: A cadaveric study in dogs

Logan M. Scheuermann DVM[1] | **Stanley E. Kim BVSc, MS, DACVS-SA**[1] | **Daniel D. Lewis DVM, DACVS**[1] | **Matthew D. Johnson DVM, MVSc, DACVS-SA**[1] | **Adam H. Biedrzycki BVSc (Hons), PhD, BSc (Hons), DACVS-LA, DECVS, PhD**[2]

[1]Department of Small Animal Clinical Sciences, College of Veterinary Medicine, University of Florida, Gainesville, Florida, USA

[2]Department of Large Animal Clinical Sciences, College of Veterinary Medicine, University of Florida, Gainesville, Florida, USA

Correspondence
Stanley E. Kim, Department of Small Animal Clinical Sciences, College of Veterinary Medicine, University of Florida, 2015 SW 16th Ave, Gainesville, FL 32610 USA.
Email: stankim@ufl.edu

Funding information
Edward DeBartolo Gift to the University of Florida

Abstract

Objective: Assess the accuracy and efficiency of reduction provided by application of plates precontoured to 3-dimensional (3D)-printed femoral bone models using a custom fracture reduction system (FRS) or intramedullary pin (IMP) to facilitate femoral minimally invasive plate osteosynthesis (MIPO) in dogs.

Study design: Experimental cadaveric study.

Sample population: Seven dog cadavers.

Methods: Virtual 3D femoral models were created using computed tomographic images. Simulated, virtual mid-diaphyseal femoral fractures were created and reduced. Reduced femoral models were 3D-printed and a plate was contoured. Custom drill guides for plate screw placement were designed and 3D-printed for the FRS. Mid-diaphyseal simulated comminuted fractures were created in cadavers, and fractures were aligned using FRS or IMP and stabilized with the precontoured plates. Number of fluoroscopic images acquired per procedure and surgical duration were recorded. Computed tomographic scans were repeated to assess femoral length and alignment.

Results: Compared to the preoperative virtual plan, median change in femoral length and frontal, sagittal, and axial alignment was less than 3 mm, 2°, 3°, and 3° postoperatively, respectively, in both reduction groups. There was no difference in length or alignment between reduction groups ($P > .05$). During FRS, fewer fluoroscopic images were taken ($P = .001$), however, surgical duration was longer than IMP procedures ($P = .011$).

Conclusion: Femoral alignment was accurate when using plates precontoured to 3D printed models, regardless of reduction method.

Clinical significance: Accurate plate contouring using anatomically accurate models may improve fracture reduction accuracy during MIPO applications. Custom surgical guides may reduce fluoroscopy use associated with MIPO.

The results of this study were presented in podium format at the Sixth World Veterinary Orthopaedic Congress and 49th Annual Veterinary Orthopedic Society Conference. Snowmass, Colorado. February 5-12, 2022.

1 | INTRODUCTION

Minimally invasive plate osteosynthesis (MIPO) is an advancement in biologic osteosynthesis, developed to limit iatrogenic soft tissue trauma.[1] By utilizing indirect fracture reduction techniques and remote plate insertional incisions, MIPO aims to preserve the local fracture environment. In dogs, MIPO has resulted in improved preservation of periosteal perfusion and equivalent or shorter time to union when compared to open reduction and internal fixation.[2–4]

Obtaining acceptable alignment during MIPO applications can be challenging.[5] Closed indirect reduction of femoral fractures is especially problematic due to the abundant surrounding musculature.[6,7] Several indirect fracture reduction techniques have been described to facilitate MIPO applications.[5,8–10] In a retrospective case series, 10% of femoral fractures stabilized via MIPO performed without intraoperative imagining required immediate surgical revision.[9] Use of fluoroscopy to assess alignment and implant placement intraoperatively may reduce the risk of complications during MIPO applications, but exposes the surgical team to ionizing radiation.

Virtual surgical planning and 3-dimensional (3D) printing are gaining interest in veterinary orthopedic surgery and the application of custom surgical guides to facilitate indirect fracture reduction during MIPO has been described.[11,12] One case report described utilizing MIPO with 2 custom surgical guides and an alignment jig for a cat with a comminuted mid-diaphyseal humeral fracture, and near-anatomic alignment was achieved.[11] Similarly, a custom 3D printed reduction system resulted in excellent reduction in dog cadavers with simulated tibial fractures.[12]

The objectives of this study were to (1) develop and describe a fracture reduction system (FRS) designed to mitigate the challenges of indirect femoral fracture reduction and (2) assess the efficiency and accuracy of reduction using accurately precontoured plates and either the FRS or placement of an intramedullary pin (IMP). We hypothesized that FRS would reduce the duration of surgery, require fewer fluoroscopic images, and produce superior alignment when compared to IMP.

2 | MATERIALS AND METHODS

2.1 | Surgical planning and 3D printing

Seven skeletally mature, mixed-breed dogs weighing 19 to 25 kg, recently euthanized for reasons unrelated to this study, were acquired. This study was approved by the University of Florida institutional animal care and use committee (study #202111344). Cadavers were frozen at −30 °C and thawed to room temperature prior to acquiring computed tomographic (CT) images of both pelvic limbs. Cadavers were placed in dorsal recumbency with both pelvic limbs extended. Both pelvic limbs of each cadaver were imaged using a slice thickness of 0.5 mm and 0.3 mm slice overlap (Aquilion Prime S computed tomography scanner, Canon Medical Systems USA, Tustin, California). Cadavers were included if no osseous abnormalities were appreciated on the CT images. The bone algorithm volumetric data Digital Imaging and Communications in Medicine (DICOM) files were imported into an image processing software program (Mimics, Materialize NV, Leuven, Belgium) and transformed into 3D models. The images were segmented using the program's predefined bone threshold (ie, 226-3071 Hounsfield units).[13] After segmentation, stereolithography (STL) files for both femurs were exported to a biomodelling software program (3-matic, Materialize NV). Right and left femurs were randomly assigned to 1 of 2 reduction groups using an online random number generator (https://www.random.org). In one group, an IMP and precontoured plate were used for fracture reduction while in the other group, a custom fracture reduction system (FRS) and precontoured plate were applied.

In both groups, a simulated diaphyseal femoral osteotomy was created virtually and the distal femoral segment was angulated in the sagittal plane, reducing distal femoral procurvatum to facilitate IMP and plate placement. Models of the virtually aligned femurs were printed (White Resin or BioMed Amber Resin, Formlabs, Sommerville, Massachusetts) using a stereolithography 3D printer (Form 3BL, Formlabs) and cured according to the manufacturer's guidelines.[14] A 3.5 mm locking compression plate (LCP; DePuy Synthes, West Chester, Pennsylvania) or a 3.5 mm limited contact dynamic compression plate (LC-DCP; DePuy Synthes) was contoured to conform to the lateral surface of each femoral model until subjectively well contoured by the primary surgeon (SEK). Plate length was chosen at the discretion of the primary surgeon to extend from the proximal aspect of the greater trochanter to the distal femoral metaphysis.

For the FRS group, an indirect fracture reduction system was specifically designed, which consisted of reduction bolts, a suture tensioner, and a suture twister. Cerclage tape threaded into the reduction bolts, positioned in predrilled screw holes, could be tensioned to draw the bone segment towards the precontoured plate. The reduction bolts had a smooth shaft and a slotted cylindrical head (Figure 1A). The suture tensioner was cylindrical and tapered at the base to accept the head of the reduction bolts. The tensioner had 2 slots to accept

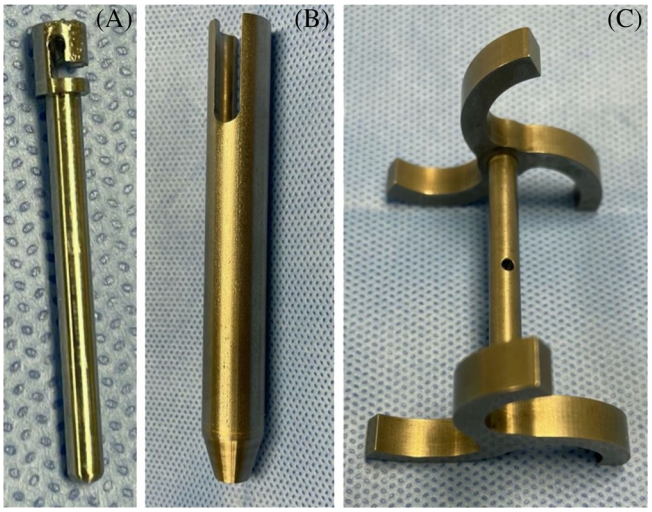

FIGURE 1 The suture tensioning system. (A) Specifically designed reduction bolt. (B) Suture tensioner. (C) Suture twister

the center rod of the suture twister (Figure 1B). The suture twister consisted of a central rod with a transverse central cannulation and 3 arms protruding from each end rod (Figure 1C).

Custom surgical drill guides were designed and printed for use in the FRS group. The guides had a 15 mm thick base with an undersurface that conformed to each femoral specimen's lateral trochanteric region or lateral condylar topography. The guides were printed and cured as described for the femoral bone models. The precontoured plate was applied to the bone model, and bicortical plate screw holes were drilled in the trochanteric and distal metaphyseal regions of the femoral model. The plate was then removed from the model, and the 3D-printed surgical guides were applied to their position of optimal fit. Corresponding holes were drilled in the custom surgical guides by drilling through the holes in the femoral models from medial-to-lateral and through the custom guides (Figure 2).

2.2 | Surgical technique

All procedures were performed by a board-certified small animal surgeon (SEK). Use of fluoroscopy was permitted as required at any stage of the procedure in either group to assess femoral alignment and implant placement. In both groups, a medial approach was created at the level of the mid femoral diaphysis and a comminuted mid-diaphyseal femoral fracture was created via multiple osteotomies using an oscillating saw. The incision was closed in a single layer. Lateral proximal and distal plate insertional incisions were made and an epiperiosteal tunnel was developed.[15]

In the FRS group, the 3D-printed guides were applied to their positions of optimal fit on the proximal and distal femur. Using the 3D printed guides, with the predrilled holes as drill guides, a 2.5 mm twist drill bit was used to create 3 or 4 bicortical holes in the major proximal and distal femoral segments. The 3D-printed guides were removed and the precontoured plate was inserted through the epiperiosteal tunnel and affixed to the proximal bone segment with 3.5-mm cortical screws. Reduction bolts were placed in the proximal- and distal-most holes in the distal femoral segment. Braided suture-tape (2 mm FiberTape, Arthrex Vet Systems, Naples, Florida) was passed around the femoral diaphysis in a double-loop configuration at the level of each bolt and passed through the slot in the bolt head, the corresponding plate hole, and secured in the suture tensioning device. The suture was tensioned, drawing the fracture segment to the plate until the head of each bolt was captured into the corresponding plate hole, thus aligning the fracture. Tension was maintained on the suture to maintain fracture reduction (Figure 3). A 3.5 mm cortical screw was placed through the empty predrilled hole in the distal femoral segment. The reduction bolts and suture were removed and 3.5 mm cortical screws were placed in the remaining vacated holes.

In the IMP group, a 2.8-3.2 mm Steinmann pin was inserted in normograde fashion. Insertion of the pin into the distal segment was performed under fluoroscopic guidance while manipulating the segment using bone holding forceps. After the fracture was aligned, the precontoured plate was placed within the epiperiosteal tunnel and affixed to the major proximal and distal bone segments with 3.5 mm cortical screws.

During all procedures, the number of fluoroscopic images acquired and surgical times were recorded. Postoperative CT scans of both pelvic limbs were obtained using the same technique as the preoperative images. Metal artifact was reduced using the single energy metal artifact reduction reconstruction technique (Canon Medical Systems USA).[16–18] The bone algorithm volumetric DICOM files were imported into modeling software (Mimics, Materialize NV) for segmentation and 3D file transformation. The STL files of both virtual femoral models were exported to 3-matic (Materialize NV). The preoperative virtually planned and postoperative femoral length, frontal plane alignment,[19] sagittal plane alignment,[20] and axial plane alignment were measured.[21] Preoperative and postoperative length and alignment data were compared within and between reduction groups. Postoperative femoral length as well as frontal, sagittal, and axial plane alignment were defined as near-anatomic, acceptable, or unacceptable based on our clinical experience. Near-anatomic reduction was defined as

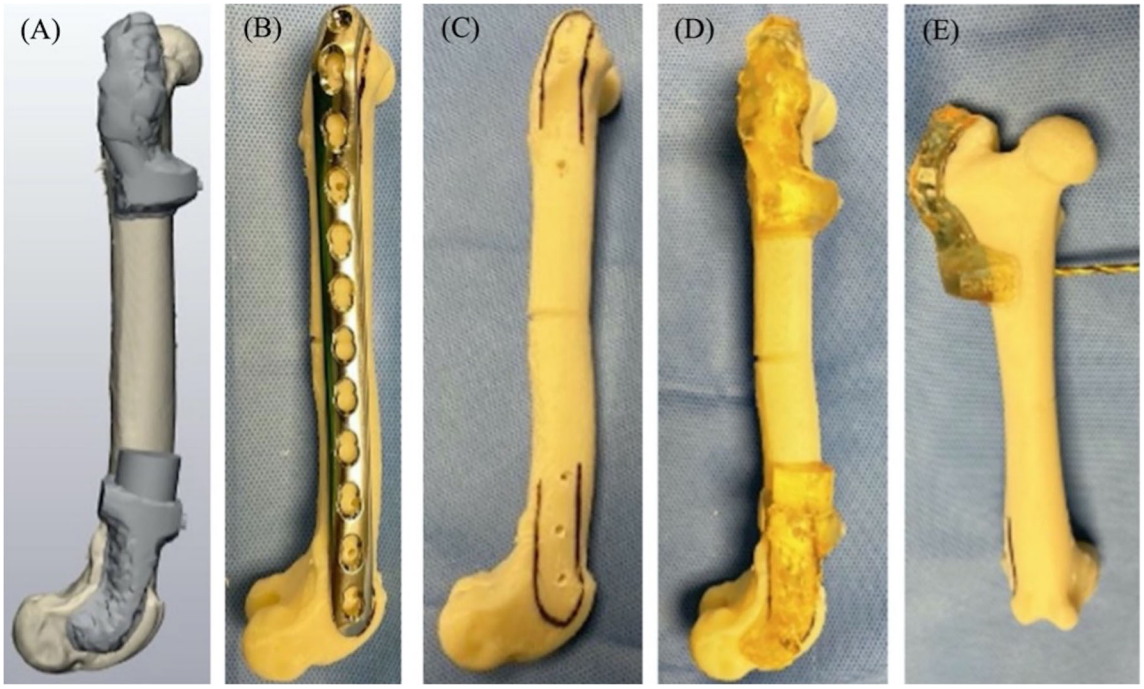

FIGURE 2 Representative step-by-step images of the custom fracture reduction system preparation. (A) Lateral view of a preoperative virtual femur model with custom guides contoured to the lateral femoral cortex. (B) A precontoured plate applied to the lateral surface of a 3D-printed femoral model. (C) Lateral view of a 3D-printed femoral model with holes drilled at locations corresponding to precontoured plate holes. (D) Lateral view of 3D-printed femoral model with custom 3D-printed guides in their positions of optimal fit. (E) Proximal-to-distal view of a 3D-printed femoral model with a proximal custom drill guide placed in its position of optimal fit. A 2.7 mm twist drill bit was used to drill holes in the drill guides corresponding to the preexisting holes in the femoral model. Holes were drilled from medial to lateral through predrilled holes

<10 mm change in femoral length, <5° change in frontal or sagittal alignment, and <10° change in axial alignment. Acceptable reduction was defined as between 10-20 mm change in length, 5°-15° change in frontal or sagittal alignment, and 10°-25° change in axial alignment. Unacceptable reduction was defined as >20 mm change in length, >15° change in frontal or sagittal alignment, or >25° change in axial alignment.

The number of fluoroscopic images taken per procedure and surgical duration were compared between groups using the nonparametric Mann-Whitney *U*-test. Differences in preoperative and postoperative length and alignment within and between reduction groups were tested using the Wilcoxon signed-rank test to account for the paired specimens. A *P*-value of <.05 was considered statistically significant. An a priori power analysis was not performed. Data are presented as median and range.

3 | RESULTS

Fewer intraoperative fluoroscopic images were acquired ($P = .001$) during FRS MIPO procedures than during IMP MIPO procedures. Surgical time, however, was longer when using the FRS ($P = .01$; Table 1).

Femoral length was shorter postoperatively, relative to the preoperative virtual plan, in the IMP group by a median of 2.3 mm (range −9.0 to 1.5 mm; $P = .03$; Figure 4). Reduction utilizing the FRS resulted in femoral length that was not different from the preoperative virtual plan with a median discrepancy of −0.6 mm (range −4.7 to 1.4 mm; $P = .40$). Postoperative femoral length was deemed near-anatomic in all cases, regardless of reduction method, as all femurs had less than a 10 mm change in length. There was no difference in the change of femoral length ($P = .24$) from the virtual plan to postoperative length between reduction groups.

Postoperative frontal plane alignment (Figure 5) was not different in the FRS ($P = .46$) or the IMP group ($P = .13$) when compared to the preoperative virtual plan with median discrepancies of −0.1° (range −4.2 to 2.9°) and −0.7° (range −2.2 to 1.9°), respectively. In all femurs, frontal plane alignment was deemed near-anatomic in both reduction groups, as all femurs had less than a 5° discrepancy in frontal plane alignment. There was no difference in frontal plane alignment between the FRS or IMP groups ($P = .87$).

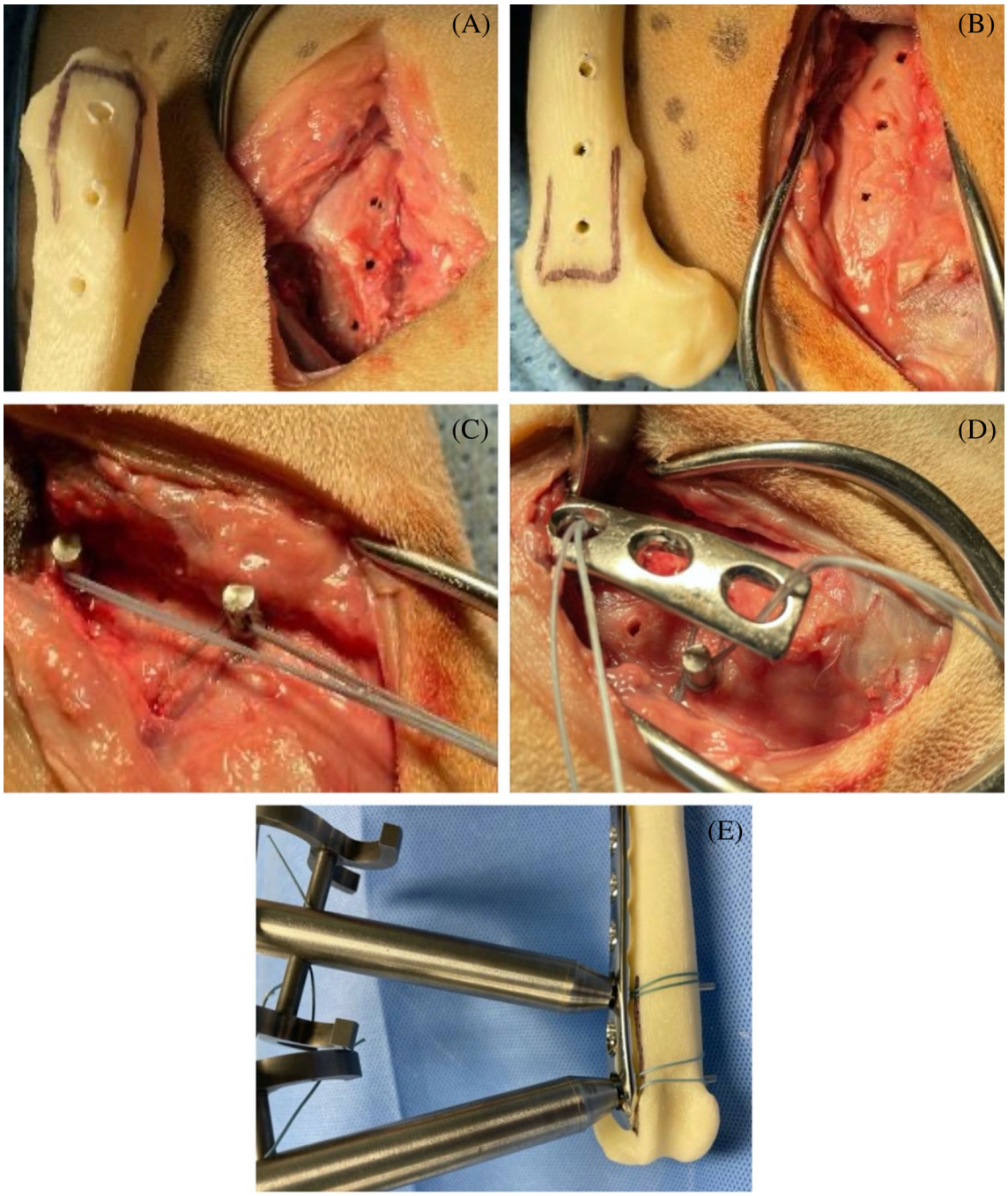

FIGURE 3 Application of the fracture reduction system. (A-B) Using the custom surgical guide, bicortical holes in the major proximal (A) and distal (B) femoral segments that corresponded to the precontoured plate holes. (C) Specifically designed reduction bolts were placed in the proximal- and distal-most holes of the distal fracture segment. Suture-tape was passed around the femur in a double loop configuration and passed through the slot in the head of the bolts. (D) A plate was affixed to the proximal femoral segment and suture-tape was passed through corresponding plate holes. (E) Suture-tape was passed through the suture tensioner and suture twister. The suture-tape was tensioned to distract and align the distal fracture segment

Femoral fracture reduction utilizing the FRS resulted in increased recurvatum relative to the preoperative virtual plan ($P = .03$) by a median of 2.9° (range −0.9 to 4.6°; Figure 6). Postoperative sagittal plane alignment was not different from the preoperative virtual plan in the IMP ($P = .31$) with a median change of 2.1° of procurvatum (range −4.1 to 3.7°). Sagittal alignment was considered near-anatomic in both reduction groups, as all femurs had less than 5° change in angulation. Sagittal alignment was not different between the FRS and IMP groups ($P = .06$).

TABLE 1 Median (range) of the number of fluoroscopic images acquired and surgical duration

	IMP	FRS	*P*
Fluoroscopic images	26 (18–47)	7 (5–9)	.001
Surgical duration (minutes)	29 (25–50)	43 (37–71)	.011

Abbreviations: FRS, 3D-printed fracture reduction system; IMP, intramedullary pin reduction.

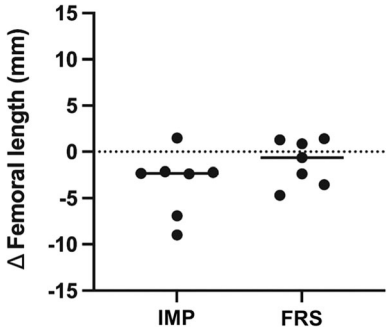

FIGURE 4 Deviation in femoral length between the virtual surgical plan and postoperative stabilized femur. The solid bar represents the median deviation in length for each reduction group. Abbreviations: IMP, intramedullary pin reduction; FRS, 3D-printed fracture reduction system; Δ, change

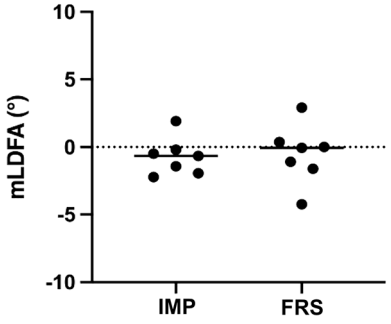

FIGURE 5 Change in distal frontal plane alignment from virtual surgical plan to postoperative alignment. Solid bar represents the median change in frontal alignment for each group. Abbreviations: IMP, intramedullary pin reduction; FRS, 3D-printed fracture reduction system; mLDFA, mechanical lateral distal femoral angle

In the FRS group, postoperative axial plane alignment was different from the preoperative virtual plan ($P = .04$) with a median change of 2.5° (range −0.7 to 7.5°; Figure 7). Axial plane alignment was not different from the preoperative virtual plan after IMP application ($P = .40$) with a median change of 2.2° (range −23.9 to 7.0°). One femur in the IMP group had acceptable alignment with 23.9° less anteversion (ie, more normoverted) postoperatively. The remainder of femurs in both groups were near-anatomic being within 10° of the preoperative

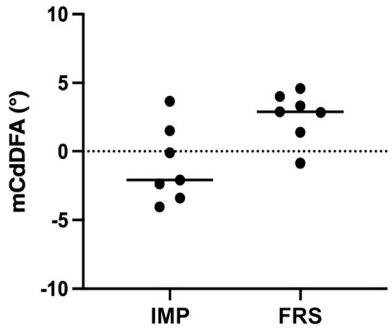

FIGURE 6 Change in sagittal plane alignment from virtual surgical plan to postoperative alignment. Solid bar represents the median change in sagittal alignment for each group. Abbreviations: IMP, intramedullary pin reduction; FRS, 3D-printed fracture reduction system; mCdDFA, mechanical caudal distal femoral angle

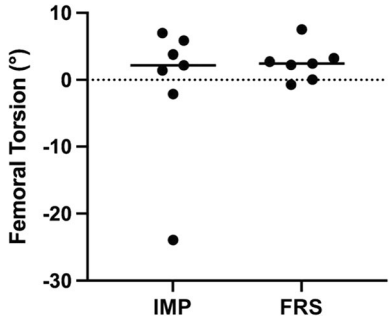

FIGURE 7 Change in axial plane alignment from virtual surgical plan to postoperative alignment. Solid bar represents the median change in axial alignment for each group. Abbreviations: IMP, intramedullary pin reduction; FRS, 3D-printed fracture reduction system

virtual plan. There was no difference in the change in axial plane alignment from the virtual plan to postoperative alignment between reduction groups ($P = .50$).

4 | DISCUSSION

We evaluated the effect of 2 fracture reduction methods for the femoral MIPO applications and partially accepted our hypotheses. Fewer fluoroscopic images were acquired during reduction with the FRS; however, surgical time was longer with FRS, and there was no difference in femoral length or frontal, sagittal, or axial alignment after reduction with the FRS or an IMP.

Application of the FRS or an IMP resulted in near-anatomic fracture reduction in all but 1 fracture in the IMP group. We also suggest that the fracture in which alignment was deemed suboptimal was sufficiently aligned to yield acceptable clinical function. The

alignment obtained with the FRS and IMP was similar to previously reported results when using indirect fracture reduction techniques for MIPO.[8,9,11,22] In a cadaveric study using a proprietary indirect reduction system (Synthes) or a temporary circular external fixator to align simulated antebrachial fractures, mean frontal and sagittal alignment was restored within ≤l° and ≤7° of normal.[22] Similarly, in a small case series of antebrachial fractures using the same proprietary reduction system to facilitate MIPO, ≤5° of deviation in postoperative frontal and sagittal alignment was reported.[8] In a clinical case series of 20 femoral fractures stabilized by MIPO performed without fluoroscopy, alignment was considered clinically acceptable in all cases, although alignment parameters were incompletely reported.[9] We partially ascribe accurate reduction in our study to fabrication of anatomic 3D-printed femoral models and accurate precontouring of plates in both reduction groups. The use of intraoperative fluoroscopy may also have contributed to similarity in final alignment as intraoperative adjustments in reduction were permitted.

Fewer intraoperative fluoroscopic images were taken during FRS facilitated procedures. Fluoroscopy is very useful when performing closed intramedullary rod placement,[6,23] particularly to help ensure that the pin has been properly seated in the distal femoral segment. Consequently, more intraoperative images were obtained during IMP facilitated procedures. In one clinical case series, immediate revision surgery was required in 10% of femoral MIPO procedures performed without fluoroscopy.[9] When the FRS was used in our study, fluoroscopic images were typically taken towards the end of the procedures to verify final implant placement and alignment. As the femur is the most common long bone fractured in cats and dogs and may require greater radiation exposure for proper image quality, the use of custom surgical guides to facilitate alignment of these injuries may have an impact limiting ionizing radiation exposure to personnel during MIPO.[24]

The median duration of surgery when using the FRS was 14 min longer than in the IMP procedures. Prolonged surgical time in the FRS reduction group was attributed to the multistep process required to deploy the reduction system, including the application of the cerclage tape and carefully fitting the drill guides to the proper location. Subjectively, the prototype suture tensioning system was cumbersome and we would not currently recommend its use in clinical cases. Aspects of FRS application that were inefficient included difficulty passing the FiberWire around the femur and through the suture tensioning system. A double loop of FiberWire was placed around the femur using a wire passer; however, securing the FiberWire to the bolt and through the suture tensioning system was relatively time consuming. To limit the difficulty placing the FiberWire, placing a toggle through the predrilled femoral holes may allow for more efficient fracture reduction, although this may necessitate leaving the toggle on the medial aspect of the femur. The suture tensioning system was also bulky and could be improved with a mechanism to lock the tension created during fracture reduction while placing the initial screw in the distal fracture segment. While not included in the surgical times, the FRS also required additional preoperative time, equipment, resources, and expertise to design, fabricate and prepare the 3D-printed surgical guides to use as drill guides.

Limitations of this study include its small sample size and lack of an a priori power analysis. Sample size was influenced by budget and time constraints and may have resulted in type II errors, particularly between reduction groups. Additionally, increasing the sample size may result in greater variability in final fracture reduction and alignment in the IMP group compared to the FRS group, as the custom surgical reduction system theoretically reduces the subjectivity and potential for inconsistencies in fracture reduction and realignment when using an IMP. Fracture reduction was classified as near-anatomic, acceptable, or unacceptable based on our clinical experience, as we are unaware of criteria for defining acceptable femoral fracture reduction. In this study, ranges for change in femoral length and alignment were used; however, using a range of acceptable joint orientation angles may better define acceptable postoperative alignment. Defining acceptable and unacceptable changes in femoral alignment after fracture reduction and alignment warrants further research. The cadaveric nature of this study also limits the ability to directly translate our results to clinical cases. Alternative fracture configurations, muscle contraction, and early callus formation would likely make reduction more difficult with both reduction methods. The FRS, however, was designed to overcome muscle tension during fracture reduction and thus the current study design may not have revealed the full benefits of the system. Finally, for simplicity, we used the ipsilateral femur for all preoperative planning. Clinically, however, planning from the intact contralateral femur may be preferred. We do not believe this limitation is of major concern because we subjectively did not note any asymmetry in bone morphology.

In conclusion, use of precontoured plates based on anatomic 3D-printed models, in conjunction with either a custom FRS or an IMP, resulted in accurate femoral MIPO fracture reduction. Custom surgical guides and FRS was associated with less exposure to ionizing radiation to the surgical team and may stimulate future development of customized systems to aid in indirect fracture reduction to facilitate MIPO applications.

AUTHOR CONTRIBUTIONS

Scheuermann LM, DVM: Study design, data collection, statistical analysis and interpretation, and manuscript preparation and revision. Kim SE, BVSc, MS, DACVS-SA: Conceptualization, Study design, data collection, statistical analysis and interpretation, and manuscript preparation and revision. Lewis DD, DVM, DACVS: Study design, manuscript revision. Johnson MD, DVM, MVSc, DACVS-SA: manuscript revision. Biedrzycki, BSc (Hons), BVSc (Hons), MRCVS, DACVS-LA, DECVS, PhD: manuscript revision. All authors approved the final version of the submitted article.

FUNDING INFORMATION

This study was funded by the Edward DeBartolo Gift to the University of Florida.

CONFLICT OF INTEREST

The authors declare no conflicts of interest related to this report.

REFERENCES

1. Krettek C, Schandelmaier P, Miclau T, Tscherne H. Minimally invasive percutaneous plate osteosynthesis (MIPPO) using the DCS in proximal and distal femoral fracture. *Injury*. 1997;28-(SUPPL.1):20-30. doi:10.1016/s0020-1383(97)90112-1 A20, A30.
2. Garofolo S, Pozzi A. Effect of plating technique on periosteal vasculature of the radius in dogs: a cadaveric study. *Vet Surg*. 2013;42(3):255-261. doi:10.1111/j.1532-950X.2013.01087.x
3. Pozzi A, Risselada M, Winter MD. Assessment of fracture healing after minimally invasive plate osteosynthesis or open reduction and internal fixation of coexisting radius and ulna fractures in dogs via ultrasonography and radiography. *J Am Vet Med Assoc*. 2012;241(6):744-753. doi:10.2460/javma.241.6.744
4. Pozzi A, Hudson CC, Gauthier CM, Lewis DD. Retrospective comparison of minimally invasive plate osteosynthesis and open reduction and internal fixation of radius-ulna fractures in dogs. *Vet Surg*. 2013;42(1):19-27. doi:10.1111/j.1532-950X.2012.01009.x
5. Guiot LP, Guillou RP, Déjardin LM. Minimally invasive percutaneous medial plate-rod osteosynthesis for treatment of humeral shaft fractures in dog and cats: surgical technique and prospective evaluation. *Vet Surg*. 2019;48(S1):O41-O51. doi:10.1111/vsu.13134
6. Peirone B, Rovesti GL, Baroncelli AB, Piras LA. Minimally invasive plate osteosynthesis fracture reduction techniques in small animals. *Vet Clin North Am Small Anim Pract*. 2020;50(1):23-47. doi:10.1016/j.cvsm.2019.08.002
7. Pozzi A, Lewis DD, Scheuermann LM, Castelli E, Longo F. A review of minimally invasive fracture stabilization in dogs and cats. *Vet Surg*. 2021;50(S1):O5-O16. doi:10.1111/vsu.13685
8. Townsend S, Lewis DD. Use of the minimally invasive reduction instrumentation system for facilitating alignment and reduction when performing minimally invasive plate osteosynthesis in three dogs. *Case Rep Vet Med*. 2018;2018:23-30. doi:10.1155/2018/2976795
9. Cabassu J. Minimally invasive plate osteosynthesis using fracture reduction under the plate without intraoperative fluoroscopy to stabilize diaphyseal fractures of the tibia and femur in dogs and cats. *Vet Comp Orthop Traumatol*. 2019;32(6):475-482. doi:10.1055/s-0039-1693413
10. Hudson CC, Lewis DD, Pozzi A. Minimally invasive plate osteosynthesis: radius and ulna. *Vet Clin North Am Small Anim Pract*. 2020;50(1):135-153. doi:10.1016/j.cvsm.2019.08.006
11. Oxley B. A 3-dimensional-printed patient-specific guide system for minimally invasive plate osteosynthesis of a comminuted mid-diaphyseal humeral fracture in a cat. *Vet Surg*. 2018;47(3):445-453. doi:10.1111/vsu.12776
12. Johnson MD, Lewis DD, Sutton WA, et al. Efficacy of two reduction methods in conjunction with 3-D-printed patient-specific pin guides for aligning simulated comminuted tibial fractures in cadaveric dogs. *Am J Vet Res*. 2022;83(9):1-10. doi:10.2460/ajvr.21.12.0215
13. Comrie ML, Monteith G, Zur LA, Oblak M, Phillips J, James FMK. The accuracy of computed tomography scans for rapid prototyping of canine skulls. *PLoS One*. 2019;14(3):1-10. doi:10.1371/journal.pone.0214123
14. Formlabs. Form Cure Manual. Sommerville, MA. 2019. https://media.formlabs.com/m/239b1aa5006cf5ff/original/-ENUS-Form-Cure-Manual.pdf. Accessed June 15, 2021.
15. Pozzi A, Lewis DD. Surgical approaches for minimally invasive plate osteosynthesis in dogs. *Vet Comp Orthop Traumatol*. 2009;22(4):316-320.
16. Wei F, Li J, Zhou C, et al. Combined application of single-energy metal artifact reduction and reconstruction techniques in patients with Cochlear implants. *J Otolaryngol Head Neck Surg*. 2020;49(1):1-9. doi:10.1186/s40463-020-00462-1
17. Yasaka K, Kamiya K, Irie R, Maeda E, Sato J, Ohtomo K. Metal artefact reduction for patients with metallic dental fillings in helical neck computed tomography: comparison of adaptive iterative dose reduction 3D (AIDR 3D), forward-projected modelbased iterative reconstruction solution (FIRST) and AIDR 3D with single-energy metal artefact reduction (SEMAR). *Dentomaxillofac Radiol*. 2016;45(7):1-7. doi:10.1259/dmfr.20160114
18. Kawahara D, Ozawa S, Yokomachi K, et al. Metal artifact reduction techniques for single energy CT and dual-energy CT with various metal materials. *BJR|Open*. 2019;1(1):1-7. doi:10.1259/bjro.20180045
19. Tomlinson J, Fox D, Cook JL, Keller GG. Measurement of femoral angles in four dog breeds. *Vet Surg*. 2007;36(6):593-598. doi:10.1111/j.1532-950X.2007.00309.x
20. Peterson JL, Torres BT, Hutcheson KD, Fox DB. Radiographic determination of normal canine femoral alignment in the sagittal plane: a cadaveric pilot study. *Vet Surg*. 2020;49(6):1230-1238. doi:10.1111/vsu.13465
21. Serck BM, Karlin WM, Kowaleski MP. Comparison of canine femoral torsion measurements using the axial and biplanar methods on three-dimensional volumetric reconstructions of computed tomography images. *Vet Surg*. 2021;50(7):1518-1524. doi:10.1111/vsu.13700

22. Gilbert ED, Lewis DD, Townsend S, Kim SE. Comparison of two external fixator systems for fracture reduction during minimally invasive plate osteosynthesis in simulated antebrachial fractures. *Vet Surg*. 2017;46(7):971-980. doi:10.1111/vsu.12687
23. Guiot LP, Déjardin LM. Perioperative imaging in minimally invasive osteosynthesis. *Vet Clin North Am Small Anim Pract*. 2020;50(1):49-66. doi:10.1016/j.cvsm.2019.08.003
24. Unger M, Montavon PM, Heim UFA. Classification of fractures of long bones in the dog and cat: introduction and clinical application. *Vet Comp Orthop Traumatol*. 1990;03(2):41-50. doi: 10.1055/s-0038-1633228

How to cite this article: Scheuermann LM, Kim SE, Lewis DD, Johnson MD, Biedrzycki AH. Minimally invasive plate osteosynthesis of femoral fractures with 3D-printed bone models and custom surgical guides: A cadaveric study in dogs. *Veterinary Surgery*. 2022;1-9. doi:10.1111/vsu.13925